Nugroho, Robertus Wahyu N.; Outinen, Marko; Toikkanen, Outi; Heino, Antti; Sawada, Daisuke; Rojas, Orlando J.

Effect of water activity on the functional, colloidal, physical, and microstructural properties of infant formula powder

Published in:
Journal of Colloid and Interface Science

DOI:
10.1016/j.jcis.2020.10.069

Published: 15/03/2021

Document Version
Peer-reviewed accepted author manuscript, also known as Final accepted manuscript or Post-print

Journal Pre-proofs

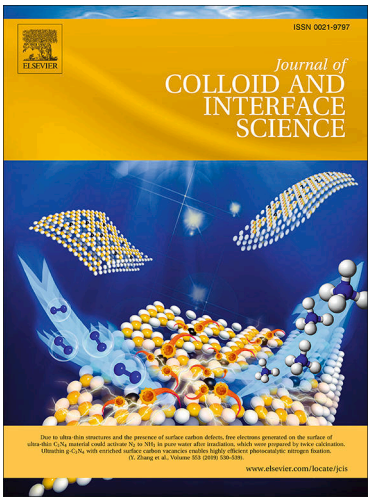

Regular Article

Effect of water activity on the functional, colloidal, physical, and microstructural properties of infant formula powder

Robertus Wahyu N. Nugroho, Marko Outinen, Outi Toikkanen, Antti Heino, Daisuke Sawada, Orlando J. Rojas

PII: S0021-9797(20)31409-0
DOI: https://doi.org/10.1016/j.jcis.2020.10.069
Reference: YJCIS 27100

To appear in: *Journal of Colloid and Interface Science*

Received Date: 19 March 2020
Revised Date: 18 October 2020
Accepted Date: 19 October 2020

Please cite this article as: R.W.N. Nugroho, M. Outinen, O. Toikkanen, A. Heino, D. Sawada, O.J. Rojas, Effect of water activity on the functional, colloidal, physical, and microstructural properties of infant formula powder, *Journal of Colloid and Interface Science* (2020), doi: https://doi.org/10.1016/j.jcis.2020.10.069

Effect of water activity on the functional, colloidal, physical, and microstructural properties of infant formula powder

Robertus Wahyu N. Nugroho[a,], Marko Outinen[b,*], Outi Toikkanen[b], Antti Heino[b], Daisuke Sawada[a], Orlando J. Rojas[a,c*]*

[a]*Department of Bioproducts and Biosystems, School of Chemical Engineering, Aalto University, Vuorimiehentie 1, Espoo, PO Box 16300, FI-00076 Aalto, Finland*

[b]*Valio, Ltd, R&D Centre, P.O. Box 30, FI-00039 Valio, Finland*

[B]*ioproducts Institute, Departments of Chemical and Biological Engineering, Chemistry and Wood Science, The University of British Columbia, 2360 East Mall, Vancouver, BC V6T 1Z3, Canada*

**Corresponding authors: rnugroho@kth.se; marko.outinen@valio.fi; orlando.rojas@ubc.ca*

Abstract

We report on the physicochemical changes of infant formula (IF) powder and its macronutrients (lactose, fat, and proteins) under given storage conditions. Colloidal (particle size distribution, emulsion stability and sedimentation), morphological (scanning electron microscopy), thermal (differential scanning calorimetry), structural (synchrotron X-ray Diffraction) as well as surface and chemical (X-ray Photoelectron and Fourier transform infrared spectroscopies) data were used to elucidate the main cause-effect relationships for microstructural, functional, and other properties of the IF powder. The wetting behavior of the powder was found to be significantly affected by water activity (a_w) during storage (a_w in the range between 0.24 and 0.42). At the highest a_w ($a_w = 0.42$), lactose crystallization and fat migration took place, leading to changes on the surface of the particles that reduced water wetting. We propose possible mechanisms to explain the observations, associated with changes in protein conformation.

Interestingly, no major changes in the pH and colloidal characteristics, including particle size and distribution, stability and sedimentation were observed in the reconstituted IF powder upon storage for 6 weeks. The results indicated a negligible contribution from possible Maillard reactions. We propose leading microstructural and wetting characterization to troubleshoot changes in the quality of IF powder, most relevant from the perspective of reconstitution after storage.

Keywords: infant formula; dairy colloids; storage; water activity; functional and physical properties; microstructure

1. Introduction

Infant formula (IF) is typically presented as a liquid or as a powder. The IF powder form is valuable if one considers factors, such as storage space, stability, handling cost, and shelf-life [1]. However, when an IF powder is stored at high relative humidity (RH), deteriorative microstructural changes might occur, involving lactose and fat, thereby affecting functionality [2]. When exposed to environmental changes upon storage, amorphous lactose experiences an irreversible transition to a crystalline phase [3-5]. Lactose crystallization in the powder has been observed after two months at RH > 43 % (water activity a_w = 0.43) [6]. Such lactose crystallization further creates caking, which inhibits wetting of the milk powder [7]. As a consequence of lactose crystallization, disruption of fat globules in the powder matrices occurs, leading to fat leakage at the powder's surface under humid conditions [8, 9]. Fat on the particle surfaces further limits water transport and diffusion, decreasing powder wettability and the ability to breaking down into smaller colloidal particles [7]. Fat dominates the powder surface, even if IF powder is stored in dry condition (0 % RH) [8]. The characterization of the microstructural properties of IF powder and milk macronutrients is critical to understand the changes in functional (wettability, flowability, color, among others) as well as the colloidal (particle size distribution, emulsion stability, sedimentation), and physical (moisture content, pH, etc.) properties under the influence of the environmental conditions, for instance upon changes in humidity.

Besides wettability, changes in IF powder microstructure are expected to affect other functional properties [10, 11] such as flowability [11], color [12], and flavor [13]. In addition, Maillard reactions add to the possible color changes, for example, from white/pale yellow to brown in both whole milk (WMP) [14] and IF [6] powders. Such effect begins by condensation of lactose on proteins or lactosylation, mainly associated with changes in physical properties, for instance temperature [15] and pH [16]. Maillard reactions can accelerate at high relative humidity [5], as indicated by the more limited lactosylation that occurs in drier milk powder (2.3 % moisture compared to 5.4 %) [15].

Several approaches have been applied to monitor the changes in milk powder microstructures. McKenna, Llyod, Murno, and Singh reported on fat-protein interactions using transmission electron microscopy (TEM). They studied the clustering of fat globules and their impact in WMP solubility [17]. The WMP solubility deteriorated with the presence of casein micelles adsorbed onto the fat globules after homogenization. Confocal microscopy (CM) was used to unveil changes in IF microstructure and to identify the coalescence of free fat covering the surface of lactose crystals [8]. In addition, scanning electron microscopy (SEM) has been used to follow the morphology of IF powders upon humidification [8]. Other techniques, including Fourier transform infrared (FTIR) spectroscopy, are instrumental to study the conformational changes of milk proteins [18-20]. Upon water uptake, water can generate a local condensation at the powder surface, allowing some milk proteins to unfold. For instance, the transformations of helical and loop protein structures, to sheet and turns, have been accessed by IR spectroscopy [21].

Despite the reports available on the changes in milk powder after storage, no clear correlations are available between the microstructural features of IF powder and its functional, colloidal, and physical properties; the latter are expected to involve changes in milk macronutrients, lactose, fat and proteins. Thus, our main objective was to investigate the stability of IF powder using complementary analyses and to evaluate IF powder functional, colloidal, physical, and microstructural properties. We identify

microstructural changes in lactose, fat, and milk proteins and elucidated their effects on the functional, colloidal, and physical properties of IF powder after storage, under the influence of varying a_w. For this purpose, IF powder was stored during given time periods at a given a_w. Overall, we provide the basis for a better understanding of the mechanisms affecting the properties of IF powder equilibrated at different a_w.

2. Materials and Methods

2.1 Materials

Spray dried IF powder was obtained from Valio Ltd. (Lapinlahti, Finland). The powder was obtained to meet the standard IF for stage 1 based on the Technical Regulation of the Customs Union "On Safety of Milk and Dairy Products" (TR TS 033/2013) and nutritional needs of infants from 0-6 months. The IF powder was packaged in sealed aluminum bags for 4 months and stored at -18° C before use. The composition of the IF powder (expressed in g/100 g) included fat (milk fat:vegetable oils of 1:1) (26.3), lactose (57.8), milk proteins (casein:whey of 60:40) (11.5), ash (2.5), and moisture (1.9).

2.2 Storage conditions

Before preparing IF samples, the commercial IF powder previously stored at -18° C was equilibrated at 22° C. Twenty grams of this fresh IF powder were placed in several plastic Petri dishes ($d_{Petri\ dish}$ = 9 cm, with a powder bed thickness of ~1 cm). The samples were then placed desiccators and exposed to a given relative humidity (RH). The conditions were set at target RH using the following saturated solutions: NaOH (> 99%, Merck, Germany) (8%), CH_3COOK (99.9 %, VWR Chemicals, Belgium) (23%), $MgCl_2$ (100%, VWR Chemicals, Belgium) (33%), and K_2CO_3 (99%, Merck, Germany) (43%). The final water activity (a_w) of the samples was ~0.08; 0.23; 0.33 and 0.43, respectively (measured at 22° C, **Table 1**). Thus, in this work, we classified different a_w according to the given equilibrium relative humidity, RH. A "dry" condition was assumed for $a_w < 0.20$, while a "low humidity" condition referred to $a_w > 0.20$. In

addition, a "high humidity" condition was assumed for $a_w > 0.40$. Finally, a "very dry" state was assigned to $a_w < 0.10$. The powder stored at week 0 at $a_w = 0.10$ was used as a reference. To demonstrate the effect of a_w after a relatively short storage time, the powders were stored and characterized after 2, 4, and 6 weeks.

Powder properties

The IF powder characterization included complementary approaches to evaluate the physical, colloidal, and functional properties, as well as the microstructural changes of IF powder after storage. All analyses of the powder properties were performed in triplicate, unless stated otherwise.

2.3 Wettability

Powder wettability was measured through the wetting time as described by the International Dairy Federation (IDF) Standard 87 [22], with slight modification due to the limited amount of IF powder. A IF sample bed (13.6 g) was placed inside a metal cylinder on a glass slide covering a beaker glass filled with 100 mL water at 50° C. By pulling the slide, the sample was immediately brought into contact with the surface of warm water and the time needed for full powder submersion was recorded.

2.4 Flowability

IF powder (13 g) was inserted in a metallic drum equipped with two opened slits, as described by the GEA Niro analytical method A23a [23]. The drum was automatically rotated clockwise at 22° C and stopped after 15 min. The powder collected through the slits was weighed.

2.5 Color

Color measurement of IF samples was determined using a CR-400 chroma meter (Konica Minolta, Tokyo, Japan). Color analysis was performed under CIE (Commission Internationale de L'Eclairage) standard D65 illuminate with an angle of observation of 0°. Prior to sample characterization, the

colorimeter was calibrated using a calibration plate and the L*a*b* color space was recorded (22° C). This followed the Hunter color parameters, with L*a*b* denoting lightness (+)/darkness (-), red (+)/green (-), yellow (+)/blue (-) coordinates. To determine the browning index (BI), due to the Maillard reactions, the L*, a*, and b* values were used in the following equations, as previously described [24]:

$$p = \frac{(a^* + 1.75L^*)}{(5.645L^* + a^* - 3.012b^*)} \quad [1]$$

$$BI = \frac{[(p - 0.31)100]}{0.172} \quad [2]$$

2.6 Water activity (a_w) and moisture content (%)

The water activity of the IF powder was measured using a water activity meter (Novasina AG, Lachen, Switzerland) (**Table 1**). For moisture content, 4 g of IF sample were placed into an aluminum plate and allowed to dry at 105 °C for 5-6 min using a halogen moisture analyzer (Mettler Toledo AG, Greifensee, Switzerland).

2.7 pH

The pH of IF powder reconstituted in water was measured at 22° C using a Portamess pH meter (Knick, Berlin, Germany) equipped with a glass electrode. Prior to use, the pH meter was calibrated using a buffer solution at pH = 4 (VWR Chemicals, Belgium) and pH = 7 (VWR Chemicals, Belgium), respectively.

2.8 Instability index of reconstituted IF powder

The IF powder was initially reconstituted, as previously described in *section 2.3*, manually stirred for 60 s. The colloidal properties of the IF reconstituted powder, i.e., instability index and height of sedimentation, were determined using a LuMiSizer (L.U.M. GmbH, Berlin, Germany). The setting

parameters used for the stability measurements included a volume of 0.4 mL emulsion, 4000 rpm, time intervals of 10 and 60 s, time $_{Exp}$ 1980 s and temperature 25^{o} C. The analysis was performed in duplicate.

2.9 Colloidal particle size of reconstituted IF powder

The volume-averaged size distribution of the reconstituted IF samples was determined with a Mastersizer 2000 (Malvern Instruments, UK) using distilled water as dispersion medium. The instrument utilizes laser with a wavelength of 466 nm. The refractive indices used to calculate the size distribution were 1.46 and 1.57, for milk fat and casein, respectively. The IF sample was initially reconstituted, as previously described in *section 2.3*, and manually stirred for 60 s. Averages of four measurements were recorded. Sodium dodecyl sulfate (SDS) (> 98.5%, Sigma Aldrich, USA)/ ethylenediamine-tetra acetic acid (EDTA) (99%, Merck, Germany) system was introduced into the emulsion system to dissociate the milk proteins and determine the sizes of the fat globules. For the measurement, the emulsion was diluted with 1 % SDS at a ratio of 1:4. Subsequently, 1 mL EDTA 35 mM was added directly into the dispersion. A 40-s delay time was used in the characterization and an average of five measurements was recorded. A representative colloidal particle size distribution and volume mean diameter (VMD), d [4,3] (μm) were reported.

2.10 Morphology

The surface morphology of IF powder was determined with a JSM-7500FA scanning electron microscope (SEM) (Jeol, Japan) at accelerating voltage of 2 kV. The samples were mounted on the double-sided adhesive carbon black. Later, they were sputtered with a gold/palladium (Au/Pd) layer (Leica EM, ACE200, Germany).

2.11 Chemical characteristics

The infrared absorption of lactose, fat, and proteins in the IF samples were evaluated by Fourier Transform Infrared (FTIR) Spectroscopy using a wavenumber range of 500-4000 cm^{-1} (Unicam Mattson

3000 spectrometer, Labexchange, Burladingen, Germany). The FTIR unit was equipped with attenuated total reflectance (ATR, PIKE technologies) to provide bulk surface analysis with a depth of few microns. The FTIR spectra of the powder were obtained as averages of 16 individual scans at 4 cm^{-1} resolution. During data analysis, all the spectra of the milk components were normalized. For the spectra of lactose and fat, they were baseline-corrected, while Fourier self-deconvolution was applied for processing the milk proteins spectra.

2.12 Phase transitions

The phase transitions of lactose were assessed using synchrotron X-ray diffraction (XRD). The XRD data were collected at beamline D2AM (ESRF, Grenoble, France). The IF samples were tightly packed into a glass tube (outer diameter = 3 mm; wall thickness = 200 μm). The glass tubes were mounted on a multi-position sample holder. Wide angle X-ray scattering (WAXS) patterns were collected in the transmission mode on a flat 2D WOS detector (imXPAD, France). X-ray energy was set to 18 keV (λ = 0.688801 Å). Sample to detector distance was calibrated using Cr_2O_3 powder. The powder diffraction data were processed using pyFAI [25], a Python library for azimuthal integration of diffraction data. The diffraction profiles were obtained from the azimuthal averaging of raw 2D image after detector distortion, flat field, and polarization factor were corrected. The diffraction profiles were then processed by normalizing the incident beam intensities. The scattering contributions from air, glass tube, and sample were subtracted to get the final XRD data. Compared to other macronutrients, lactose may crystallize into various crystal forms, which can be identified by their diffraction patterns. In dairy powder, amorphous lactose undergoes phase transition into crystalline structures, such as α-lactose monohydrate, anhydrous β-lactose, anhydrous crystal with α and β in molar ratio of 5:3 and 4:1, depending on the RH and temperature [3, 26]. These crystal forms exist at diffraction angles (2θ) of (12^o - 12.6^o, 16^o - 16.4^o, and 20^o -20.4^o) and (10.3^o - 10.8^o, 20.9^o, and 21^o) for α-lactose monohydrate and anhydrous β-lactose, respectively. In addition, the peak intensity of the α/β anhydrous crystal mixture at molar ratio of 5:3 and

4:1 exists at 2θ of (19.1°, 21.1°) and (19.5°, 21.2°), respectively [3, 26, 27]. The degree of lactose crystallinity (%) was calculated by dividing the crystalline area over the total area (amorphous + crystalline) of the diffraction profiles. In addition, the peak area of lactose crystalline structures was acquired from the Gaussian fitting model.

2.13 Surface analysis

The surface fat of IF powder was characterized by X-ray Photoelectron Spectroscopy (XPS) using an AXIS Ultra electron spectrometer (Kratos Analytical, U.K). The sample was mounted on UHV-compatible carbon tape secured on the sample holder. Each IF sample was pre-evacuated overnight together with a freshly prepared pure cellulose. A filter paper sample was used as a reference [28]. XPS spectra were recorded at 100 W under neutralization. The XPS spectral analysis was performed using CasaXPS software. The surface chemical composition was determined from wide scans. The data were further evaluated from high resolution C 1s, O 1s and N 1s regions. Each sample was characterized in triplicate. Note: the XPS analysis area was <1 mm and the penetration depth < 5 nm. To calculate the XPS surface composition of milk powders we used procedures already described [29, 30]. Briefly, the relative atomic concentration of carbon, nitrogen, and oxygen was quantified and used in a matrix (Eq. 3, 4, and 5) accounting for the surface content and assuming the three main compounds in the sample, i.e., lactose (L), fat (F), and protein (P):

$$I^C = \alpha L I^{C_L} + \alpha' F I^{C_F} + \alpha'' P I^{C_P} \quad [3]$$

$$I^N = \alpha L I^{N_L} + \alpha' F I^{N_F} + \alpha'' P I^{N_P} \quad [4]$$

$$I^O = \alpha L I^{O_L} + \alpha' F I^{O_F} + \alpha'' P I^{O_P} \quad [5]$$

where I^C, I^N, and I^O are the calculated mole fractions of carbon, nitrogen, and oxygen on the sample surface. These values were obtained from the area of the C1s, N1s, and O1s of the XPS peaks. I^{C_L}, I^{C_F},

and $I^{C_P}$are the mole fraction of carbon in lactose, fat, and protein, respectively. I^{O_L}, I^{O_F}, and I^{O_P} are the mole fractions of oxygen for the respective component. Similarly, the mole fractions of nitrogen in lactose, fat, and milk proteins are I^{N_L}, I^{N_F}, and I^{N_P}. The lactose, fat, and milk protein concentration at the powder surface was determined by solving the matrix (αL), $(\alpha' F)$, and (α''). Considering the atom-weight difference between carbon (12), nitrogen (14), and oxygen (16), the relative surface content was calculated on a mass basis.

2.14 Thermal properties

The thermal properties of the IF samples were determined *via* Differential Scanning Calorimetry (DSC 3+, Mettler Toledo AG, Schwerzenbach, Switzerland) using the STARe thermal analysis software. The samples (3 - 5 mg) were weighed in 40-mL aluminum pans and then heated from 20^o to 80^o followed by cooling -50^o C and, once final heating to 150^o C (heating-cooling rate of 5 K/min under N_2 atmosphere).

2.15 Statistical analysis

Differences between measurements were tested with one-way analysis of variance (ANOVA). The significance of the differences was thereafter tested with Tukey's honest significance test at $p < 0.05$. All statistical tests were performed using Minitab Statistical (LCC, Pennsylvania, USA) software.

3. Results and Discussion

3.1 Wettability, flowability, and color

Wettability is a key factor in defining powder quality for its consumption. In the context of dairy powders, the wettability refers to the ability of the material to become fully immersed in water. Under different storage conditions, the IF powder wettability was significantly poorer (increased wetting time) with increased water activity (a_w) during storage (**Figure 1a**).

The IF sample reached equilibrium during moisture sorption. Thus, no changes in IF powder wettability were observed after the 2-week intervals, indicating that the effect of a_w was dominant over the storage time (**Figure 1a**). A limited wetting of whole milk powder (WMP) has been reported, unless fat is extracted [31]. However, in our case, the reduced wettability of the IF powder in the a_w range = 0.10 - 0.32 (**Figure 1a**), cannot be explained solely by the role of fat, or more specifically, surface fat, whose concentration remained unchanged (**Figure 2**).

The IF powder flowability, expressed by the mass of collected powder, was not significantly affected by humidity in the a_w range = 0.10 - 0.32 (**Figure 1b**). Similar to the observations of powder wettability, the data indicated a negligible influence of storage time on the powder flow.

Fat has previously shown to reduce milk powder flowability. For instance, the flowability of WMP at a moisture of 3.3 g/100 g was impacted by fat for powder stored at different temperatures (10-30^o C) [32]. The melting of milk fat resulted in fat capillary bridges between solid particles [33], thus causing larger cohesive interactions, undermining flowability [32]. Once again, this phenomenon was not as relevant in our study with IF powder at a_w = 0.10 - 0.32 (**Figure 1b**). Importantly, a highly undesirable phenomenon in dairy industry, caking, took place at a_w = 0.42 after 2-week storage (in such cases flowability cannot be measured). Caking describes an initially free-flowing powder containing low moisture content that gradually forms solid lumps, forming then a hardened solid structure [34]. Such caking is expected to occur due to capillary interaction [35], thus allowing liquid bridges to form [36]. This effect can be further induced by lactose crystallization [36].

The color changes were determined by using Hunter's L* parameter (**Figure 1c**), following a previous study with WMP [37]. In addition, browning index, an indicator of Maillard reactions in foods, was calculated using Eq. 1 and 2, involving the Hunter parameters, L*, a*, and b* (**Figure 1d**). As seen in **Figure 1c**, the lightness, L*, of the IF powder showed no significant changes at a_w < 0.42 (**Figure 1c**). L* significantly decreased to lower values (darker) at a_w of 0.42 (**Figure 1c**). Similar to our finding,

lower L* was found in WMP powders, related to the early stage browning due to the Maillard reaction [38]. Lactose crystallization in milk powders at $a_w > 0.4$ is believed to induce increasing browning rates, and thus Maillard reactions [6]. However, the browning index (BI) of the stored IF powders demonstrated lower values than their respective IF reference (**Figure 1d**). Thus, the effect of a_w on color changes through BI was not measurable. As a rule of thumb, a higher index relates to a more extensive browning reaction, which correlates with high concentration of melanoidins in the powder during the final stage of reaction [16]. As noted earlier, the Hunter parameters measured for the powder contributed to the BI (Eq. 1 and 2). While L* changed, particularly at $a_w = 0.42$, the a* and b* Hunter parameters showed no significant variation in the a_w range of 0.12-0.42, signifying no major change in BI (**Figure 1d**).

3.2 Particle size distribution, pH, emulsion stability, and moisture content

The effect of a_w on the colloidal behavior of the powder upon reconstitution was investigated through particle size distribution. Monomodal colloidal particle size distributions were observed following light scattering measurements (**Figure 3a-3d**). The changes in particle size were followed to investigate colloidal interactions between the fat globules, creating larger clusters or particles and eventually causing emulsion instability.

The volume mean diameter (VMD) or d[4,3] of the reconstituted IF samples at various a_w was similar or smaller compared to that of the respective reference sample (**Figure 3e**). The individualized fat droplets, after EDTA and SDS addition (**Figure 3f**), were slightly smaller than protein-bound fat droplets during rehydration (**Figure 3e**). The fat droplets mostly indicated VMD < 1 μm. Fat droplets < 1 μm enhance emulsion stability [39, 40]. However, no significant changes in distribution profiles were observed for the individualized fat droplets from the powder after storage, in comparison to their respective reference, even after addition of EDTA and SDS. Thus, a_w did not lead to the formation of (large) fat clusters upon reconstitution of the powder that was previously stored for up to 6 weeks.

The pH upon powder reconstitution in water remained fairly constant for samples stored at given a_w and time (**Figure 4a**). The Maillard reactions, noted to occur in the a_w range of 0.4 - 0.8 [16], were influenced by pH [41, 42]. The browning rates, due to Maillard reactions, are expected to increase with pH, up to pH 10 [43, 44]. In this work, the IF samples at a_w = 0.42 did not present Maillard reactions upon reconstitution (**Figure 4a**).

The moisture content of IF powder was determined at 2-week intervals at given a_w and compared to that of the reference IF powder, **Figure 4b**. As expected, storage at given a_w influenced markedly the moisture content. The onset of moisture uptake was found to be at a_w = 0.24 and continued to rise to the highest a_w, 0.42 (**Figure 4b**). The role of lactose and protein in moisture uptake has been studied at different a_w [45, 46]. Haque and Roos indicated that lactose absorbed less water at $a_w \leq 0.23$ during storage [45]. In contrast to lactose, the role of proteins was found to be dominant at low relative pressure or a_w (0.25) [46]. Thus, we speculate that amorphous lactose was stable and absorbed less water at a_w = 0.24, while milk proteins dominated water sorption at the same a_w. Lactose was expected to absorb moisture at $a_w >$ 0.32.

To further understand associated changes after storage (**Figure 3a-3d**), the effect of a_w on other colloidal properties was investigated upon rehydration, *via* the instability index (ISI) (**Figure 4c**) and sedimentation height (**Figure 4d**) determined by centrifugation. ISI values < 0.25 indicate emulsion systems that are relatively stable. The ISI of the IF reconstituted samples did not vary significantly with a_w and storage time. Further, the sedimentation height showed no change with storage (**Figure 4d**), indicating similar insolubility index. In contrast to our finding, other authors observed that the insolubility index increased almost two-fold at a_w = 0.23 over 8 weeks [6]. This observation was associated with rapid protein denaturation [6].

3.3 Surface morphology.

As shown earlier, as far as most of the physical, colloidal, and functional properties, the IF powder stored at a_w = 0.12 behaved similar compared to the reference powder (a_w = 0.10). Thus, unless otherwise stated, these IF powders are interchangeably used to monitor the changes in the microstructure during storage, especially as a function of a_w. To elucidate the effect of a_w on the powder morphology, SEM images were acquired.

All the IF powders at a_w = 0.12 - 0.32 were spherical, agglomerated, and porous under the different storage conditions (**Figure 5a**). Similarly, the microstructure of the IF cake (a_w = 0.42) was spherical and porous. In addition, needle-like lactose crystals were abundant and covered the IF powder surface at a_w = 0.42 (**Figure 5f**). Similar to our finding, lactose crystals at the cake surface were observed by confocal laser scanning microscopy (CLSM) during storage [9]. Further, SEM images revealed changes in surface morphology at large magnification, from relatively smooth at a_w < 0.24 (**Figure 5c**) to rather rough at a_w = 0.12 - 0.32 (**Figure 5d**) and rough at a_w > 0.32 (**Figure 5e**), due to moisture sorption at week 6. Surface roughness is a factor that is expected to influence powder flowability. Compared to rough particles, those displaying smooth surfaces are generally subjected to lower friction interactions and therefore they flow more easily. Changes in the surface topography at a_w range of 0.24 - 0.32, involving the formation of surface wrinkles, did not influence powder flowability (**Figure 1b**); however, they did affect powder wettability (**Figure 1a**).

Wrinkling is common in polymeric materials where structural changes occur under external stimuli, such as solvent diffusion [47]. The interactions between water and milk proteins, during moisture uptake, are likely to induce transition in molecular conformations. The exposure of the hydrophobic amino acids or peptide bonds previously buried in the material may occur under the influence of water [48]. In addition, the previous studies revealed wrinkling at high milk protein concentration [49, 50]. Thus, in the present case, protein structure and organization might change spontaneously upon water uptake. We speculate that changes in protein conformation tracks with surface wrinkling at a_w > 0.12 at week 6, as noted earlier

(**Figure 5d** and **5e**). The presence of surface wrinkling at a_w = 0.24 (**Figure S1b,** Supplementary data) and a_w = 0.32 (**Figure S1c,** Supplementary data) was also evident earlier, at week 2, when the IF powder reached equilibrium water sorption (confirmed by moisture content analysis, **Figure 4b**).

3.4 Surface chemistry

FTIR has been previously used as a routine technique to identify the chemical changes of dairy products [18-20]. In this work, changes in the surface chemistry of lactose, fat, and protein, upon different storage conditions, were qualitatively detected using FTIR spectroscopy. Since a_w has a dominant effect compared to the storage time, we used a_w to follow the changes in the surface chemistry of IF powder after storage (**Figure 6**). Our results (IR spectroscopy at wavenumber range of 800-1200 cm^{-1} at a_w of 0.23, even after 6-month storage) rule out lactose crystallization (**Figure 6a**) [6]. However, at a_w = 0.42, we identified multiple sharp peaks, characteristic of lactose's functional groups. This indicates the formation of lactose crystals at week 6 (**Figure 6a**) as confirmed by the needle-like crystals observed by SEM (**Figure 5f**). It is worth noting that the peak absorption of amorphous and crystalline lactose overlapped at the same wavenumber range (**Figure 6a**). The C=O stretching of fat in WMP and IF powders occurs at wavenumbers in the 1700-1800 cm^{-1} range [20, 51]. After 6-week storage, the intensity of the characteristic C=O bond in fat at 1745-47 cm^{-1} decreased noticeably at a_w = 0.42, but it overlapped at a_w = 0.1 - 0.32 (**Figure 6b**). The fat reduction at a_w = 0.42 (**Figure 6d**), as detected by FTIR, might indicate fat migration, possibly through capillary action. During storage of milk powders, lactose crystallization has been found to enhance the migration of internal fat onto the powder surface [52]. However, our FTIR results did not agree with earlier reports indicating abundant surface fat (XPS) in WMP powder [53]. Obviously, XPS and FTIR have a different penetration depth (nanometers and few micrometers, respectively). In FTIR, the area determining fat concentration was detectable and larger than an ultrathin fat layer. The results indicate the that IF powder stored at a_w = 0.42 had low fat content inside the power, few microns underneath the surface. This can be taken as an indication that fat migrated

to the surface (**Figure 6b**, **6d**) and spread on the IF powder, due to lactose crystallization. Such change delayed the wettability, particularly at a_w = 0.42 (**Figure 1a**). Some of the internal fat might have also covered needle-like lactose crystals at the surface and generated ultrathin layers, event at a_w = 0.42 (XPS data, **Figure 2**).

Compared to lactose and fat, milk proteins are involved in more complex surface chemical changes with increased moisture uptake. The different amide bonds of protein, i.e., amide I, II, and III, absorb IR differently. Amide I, II, and III are assigned to the 1600-1700 cm^{-1}, 1500-1600 cm^{-1}, and 1200-1500 cm^{-1} regions, respectively [20, 54]. IR absorption of different casein secondary structures correspond to the amide I region [19]. β-turns, α-helix, random coils, and β-sheets are associated to wavenumbers of 1660-1700 cm^{-1}, 1648-1652 cm^{-1}, 1642-1648 cm^{-1}, and 1620-1640 cm^{-1}, respectively. Different from amide I region, the amide II region relates to β-turns, α-helix, and β-sheets, captured at the wavenumber range of 1555-1578 cm^{-1}, 1543-1555 cm^{-1}, and 1525-1542 cm^{-1} [19]. Importantly, the bands resolved in the amide I region, as captured by IR spectroscopy, can be related to changes in protein conformation [55], including those after heating [18].

Different secondary structures of β-lactoglobulin have been identified. The amide I region of this protein consists of β-turns, α-helix, random coils, and β-sheets at the wavenumber range of 1663-1694 cm^{-1}, 1652-1656 cm^{-1}, 1644-1646 cm^{-1}, and 1624-1637 cm^{-1}, respectively. Changes in milk protein conformations under the influence of heating have been reported [20] and we used the respective wavenumbers assigned to amide I and II of milk proteins following previous work [18-20]. After storage, and under the influence of a_w, we detected changes in milk proteins conformation, beyond those of casein or whey proteins. In order to evaluate specific changes in the protein secondary structures, the absorption peaks of amide I and II bands at 1500-1700 cm^{-1} were normalized and thereafter Fourier self-deconvoluted to resolve the overlapped peaks (**Figure 6c**). Changes in surface chemistry were used to highlight the role of milk proteins in reducing IF powder wettability at a_w = 0.24 - 0.32 (**Figure 1a**) and

to support the observed wrinkling at such a_w range (SEM, **Figure 5d** and **5e**). Our qualitative analysis demonstrated that the proportion of β-sheet at ν ~ 1525-1542 cm^{-1} (amide II) decreased with a_w (**Figure 6c**), thus indicating changes in the conformation of milk proteins upon storage. As previously noted, the amino acids or peptide bonds may be exposed to the surface under the influence of water [48]. Thus, the rearrangements of β-sheets took place due to the increased moisture uptake in the range of a_w = 0.12 - 0.32 (**Figure 6c**), with the local surface exposing amino acids with hydrophobic moieties, thereby hindering water diffusion and disrupting wetting (**Figure 1a**). Further investigation is needed to explore the rearrangement of different amino acids, which are expected to affect the wettability of the IF powder (a_w = 0.24 - 0.32).

To verify the reversible conformational changes in milk proteins, we stored the IF powder for 10 days under equilibrium RH to achieve a_w = 0.30 (**Figure S2**, Supplementary data). At a_w = 0.30, there was a clearly reduction in the proportion of β-sheet and β-turn at υ ~ 1525-1542 cm^{-1} and υ ~ 1660-1675 cm^{-1} (**Figure S2**, Supplementary data), thus indicating conformational changes in the secondary structures of the proteins. In addition, the protein's helical structures were also reduced at υ ~ 1647-1654 cm^{-1}.

In additional experiments, after reaching a_w = 0.30, the powder was immediately stored at very dry condition (a_w = 0.05). We then measured the wetting time of the powder under such condition. Interestingly, the protein secondary structures and the proportion of β-sheet, α-helix, and β-turns at a_w = 0.05 changed back to the initial values at a_w = 0.17 (**Figure S2**, Supplementary data). In addition, the wetting time of the IF powder at a_w = 0.05 (**Table S1**, Supplementary data) matched that of the IF powder stored at a_w = 0.12 (**Figure 1a**) and at a_w=0.17 (**Table S1**, Supplementary data); meanwhile, an increased wetting time was observed for the IF powder stored at a_w = 0.30 (**Table S1**, Supplementary data). Therefore, there is clear indication of conformational reversibility of milk proteins after moisture sorption-desorption cycles (**Figure S2**, Supplementary data).

3.5 Lactose crystallinity

Synchrotron XRD analyses were used to evaluate the different types of lactose crystals, in terms of their anomers. Crystalline and amorphous structures were identified by the presence of sharp and broad peaks, in XRD patterns, respectively (**Figure 7a**). However, the identification of different crystal forms in the bulk powder was not possible. At a_w = 0.12 - 0.32, a representative diffraction peak at 12 - 12.6^o indicated the presence of the α-lactose monohydrate crystals at week 6. These crystals could function as 'initial seed' to facilitate the rapid growth of α-lactose monohydrate. For the representative peak at 12.6^o, the seed crystals were already present, before the IF powder was stored (**Figure S3a**, Supplementary data). However, the presence of the seed crystals in the IF powder, a_w = 0.12 - 0.32, did not support the growth of lactose crystals during storage, as indicated by the similar crystallinity values measured for different storage times (**Figure 7b**). This finding confirms that lactose might not contribute significantly to moisture sorption in such a_w range, as previously suggested from the FTIR analysis (**Figure 6a**) and a high amount of amorphous lactose may still be present at $a_w < 0.33$ [6]. With the high moisture sorption at a_w = 0.42, the XRD peak intensity increased significantly at 2θ of 12.8^o, 16^o, and 20.3^o, corresponding to strong signals of α-lactose monohydrate (**Figure7a**). However, lower peak intensity of the same crystal was detected at a_w = 0.42 for shorter storage times (**Figure S3b** and **S3c**, Supplementary data), indicating that lactose crystallization is a time-dependent phenomenon. In addition, at a_w = 0.42, another crystal form, β-anhydrous lactose, was identified in the XRD patterns at week 6 (**Figure 7a**). At this highest a_w, the existence of the needle-like morphologies, typical of α-lactose monohydrates [56], was confirmed at the IF powder's surface (**Figure 5f**). From this observation, we hypothesize that lactose crystals might support fat migration (**Figure 6d**), thus delaying wetting of the IF powder after storage (**Figure 1a**).

3.6 Glass transition and crystallization temperature

The glass transition (T_g) (**Figure 7c**, dotted square) and crystallization (T_{cr}) (**Figure 7c**, gray arrow) temperatures of lactose decreased with increasing a_w, regardless of the storage time. This is due to the effect of water in plasticizing the amorphous lactose. The molecular mobility of lactose may increase with water uptake before crystallization. Later, this phenomenon induces the lactose molecules to form more ordered structures, that act as crystal nuclei. As moisture is absorbed on the surface of lactose crystals, the internal water in the amorphous lactose matrix is released, thereby accelerating the phase transition of lactose, from amorphous to crystalline [2]. Subsequently, a T_g was not apparent in the DSC profile at a_w = 0.42, indicating the onset of lactose crystallization [2]. This phenomenon was also followed by the absence of T_{cr} (**Figure 7c**). The disappearance of T_g and T_{cr} indicated lactose crystallization, as previously supported by the previous observation related to surface morphology (**Figure 5d**), surface chemistry (**Figure 6a**), and crystallinity (**Figure 7a**). Importantly, although needle-like features at a_w = 0.42 were abundant at week 6 (**Figure 5f**), the thermal analysis showed identical DSC profile of crystalline lactose for shorter storage times. The degree of lactose crystallinity at 12 % (**Figure 7b**) was sufficient to make T_{cr} undetectable for lactose at a_w = 0.42 at week 2 and 4, respectively. The lactose crystals at the surface, however, were less abundant at week 2 (**Figure S1d,** Supplementary data) compared to those at week 6 (**Figure 5f**), indicating time-dependent lactose crystallization. Thus, at week 2 more abundant lactose crystals might exist in the bulk of the IF cake than on the surface (**Figure S1d,** Supplementary data). Such observation can be confirmed by DSC, which showed fat leakage might have occurred at a_w = 0.42, as determined by the presence of a broad fat melting region, from -50 to +40^o C (**Figure 7c**). However, at week 6, thermal profiles supported the results from surface chemistry analyses, providing clear evidence of fat leakage in the IF powder due to fat migration (**Figure 6d**). Similar to the present finding, we observed fat leakage at a_w = 0.43 in our earlier work using confocal laser scanning microscopy CLSM [9]. However, it is worth noting that powder wettability and moisture

content could significantly change at $T_{storage} < T_g$ under the influence of different a_w. The complexity of the IF powder, however, challenges any effort to reveal conformational changes by DSC and the detection of enthalpies of protein relaxation.

4. Conclusions

Adding to previous studies on the effect of water activity (a_w) on infant formula (IF) powder [2, 4, 6, 9], this work investigated powder stability by using complementary analyses. We elucidate the fundamental role of the macronutrient present in IF powder, such as lactose, fat, and milk proteins at given water activity, a_w, upon storage for 2 to 8 weeks. The changes in physical, colloidal, functional, and microstructural properties of IF powder were followed in the context of milk proteins, not explored before. The stability of IF powder was investigated under the influence of a_w up to 6-week storage. The wettability of the IF powder underwent significant changes (a_w between 0.12 - 0.42), a phenomenon that was ascribed to the role of milk macronutrient. At low a_w (0.24 - 0.32), the morphology of powder and its surface, including wrinkling, tracked with changes in protein conformation. A decrease in the IR absorption peak of β-sheet (wavenumber range of 1525 - 1542 cm^{-1}) was observed following an increased a_w, from 0.24 to 0.32, confirming changes in protein conformation. The role of milk proteins, lactose and fat were studied with respect to microstructural changes on the IF powder and its functional properties as monitored at a_w of 0.12 - 0.42. At $a_w = 0.42$, lactose experienced phase transitions from amorphous to crystalline, as observed in previous studies [2, 4, 6, 9]. Multiple sharp IR absorption peaks at 800-1200 cm^{-1} indicated lactose crystalline structures at high a_w ($a_w = 0.42$). Needle-like structures and changes in glass transition temperature (T_g), from amorphous to crystalline lactose, were significant at $a_w = 0.42$ (FTIR, SEM and DSC). In addition, synchrotron XRD captured a significant increase in the degree of lactose crystallinity, thus confirming phase transition at $a_w = 0.42$. Lactose crystallization induced fat migration in the powder [9, 52]. A decrease in fat concentration at $a_w = 0.42$ indicated fat migration to the surface. Lactose crystals, along with fat on the surface of IF powder, deteriorated water wettability

at high a_w. Flowability was prevented at a_w = 0.42, as a result of caking. The IF powder color lightness was found to change at a_w = 0.42. In contrast to the functional properties, no changes in the colloidal behavior (particle size distribution, emulsion stability, and sedimentation) was observed upon reconstitution of IF powder at a_w =0.12-0.42. To gain better understanding of the role of milk proteins at a_w = 0.24 - 0.32, future work should consider the amino acids present on the surface of milk proteins, which are expected to affect wettability. Our results further the possibility to engineer fully wettable IF powder by combining processing parameters and formulation.

Acknowledgements

This work was funded by Valio postdoc program. OJR wishes to acknowledge support by the European Research Council (ERC) under the European Union's Horizon Research 2020 and Innovation program (ERC Advanced Grant Agreement No. 788489, ''BioElCell'') and the Canada Excellence Research Chair Initiative. We also thank the French National Research Agency (ANR) under the "Investissements d'avenir" program (grant number: ANR-11-EPQX-0010) for WAXS (WOS). The authors thank Dr. Isabelle Morfin for her assistance at the D2AM beam line and ESRF (Grenoble, France) for the provision of beam time. We are grateful to Dr. Leena-Sisko Johansson and Dr. Joseph Campbell (Aalto) for XPS experiments and Dr. Long Bai (UBC) for helpful discussions.

Conflicts of interest

The authors have declared no conflicts of interest.

Appendix Supplementary Data

Supplementary data to this article is available online free of charge.

References

[1] R. Zhu, H. Cheng, L. Li, H. R. Erichsen, M. A. Petersen, J. Soerensen, L. H. Skibsted, Int. Dairy J. 77 (2018) 1-9.

[2] T. W. Y. Tham, C. Wang, A. T. H. Yeoh, W. Zhou, J. Food Eng., 175 (2016) 117-126.

[3] M. K. Haque, Y. H. Roos, Carbohydr. Res. 340 (2005) 293-301.

[4] T. W. Y. Tham, A. T. H. Yeoh, W. Zhou, Food Chem. 219 (2017) 117-125.

[5] M. K. Thomsen, L. Lauridsen, L. H. Skibsted, J. Risbo, J. Agric. Food Chem. 53 (2005) 7082-7090.

[6] K. Li, M.W. Woo, C. Selomulya, J. Food Eng. 169 (2016) 196-204.

[7] Y. Fang, C. Selomulya, X. D. Chen, Dry. Technol. 26 (2008) 3-14.

[8] N. A. McCarthy, V. L. Gee, D. K. Hickey, A. L. Kelly, J. A. O'Mahony, M. A. Fenelon, Int. Dairy J. 29 (2013) 53-59.

[9] O. Toikkanen, M. Outinen, L. Malafronte, O. J. Rojas, Int. Dairy J. 82 (2018) 19-27.

[10] H. Cheng, R. Zhu, H. Erichsen, J. Soerensen, M. A. Petersen, L. H. Skibsted, Int. Dairy J. 73 (2017) 166-174.

[11] E. H. Kim, X. D. Chen, D. Pearce, J. Food Eng. 94 (2009) 182-191.

[12] A. Nasirpour, J. Scher, M. Linder, S. Desobry, J. Dairy Sci. 89 (2006) 2365-2373.

[13] M. N. Kim, M. Saltmarch, T. P. Labuza, J. Food Process Pres. 5 (1981) 49-57.

[14] T. T. Le, B. Bhandari, J. W. Holland, H. C. Deeth, J. Agric. Food Chem. 59 (2011) 12473-12479.

[15] F. Guyomarc'h, F. Warin, D. D. Muir, J. Leaver, Int. Dairy J. 10 (2000) 863-872.

[16] M. N. Lund, C. A. Ray, J. Agric. Food Chem. 65 (2017) 4537-4552.

[17] A. B. McKenna, R. J. Lloyd, P. A. Munro, H. Singh, Scanning 21 (1999) 305-315.

[18] X. L. Qi, C. Holt, D. McNulty, D. T. Clarke, S. Brownlow, G. R. Jones, Biochem. J. 324 (1997) 341-346.

[19] D. M. Curley, T. F. Kumosinski, J. J. Unruh, H. M. Farrell Jr, J. Dairy Sci. 81 (1998) 3154-3162.

[20] M. Ye, R. Zhou, Y. Shi, H. Chen, Y. Du, J. Dairy Sci. 100 (2017) 89-95.

[21] S. Nasser, A. Hédoux, A. Giuliani, C. Le Floch-Fouéré, V. Santé-Lhoutellier, I. de Waele, G. Delaplace, J. Sci. Food Agric. 98 (2017) 2243-2250.

[22] International Dairy Federation, Brussels, Belgium, 1979.

[23] G. Niro, A/S Niro Atomizer–GEA NIRO: Copenhagen, 109, 1978.

[24] G. R. Askari, Z. Emam-Djomeh, S. M. Mousavi, Dry. Technol. 26 (2008) 1362-1368.

[25] G. Ashiotis, A. Deschildre, Z. Nawaz, J. P. Wright, D. Karkoulis, F.E. Picca, J. Kieffer, J. Appl. Crystallogr. 48 (2015) 510-519.

[26] K. Jouppila, J. Kansikas, Y. H. Roos, Biotechnol. Prog. 14 (1998) 347-350.

[27] N. Yazdanpanah, T. A. Langrish, Dry. Technol. 29 (2011) 1046-1057.

[28] L.-S. Johansson, J. Campbell, Surf. Interface Anal. 36 (2004) 1018-1022.

[29] P. Fäldt, B. Bergenståhl, G. Carlsson, Food Struct. 12 (1993) 225-234.

[30] C. Gaiani, J. J. Ehrhardt, J. Scher, J. Hardy, S. Desobry, S. Banon, Colloids Surf. B: Biointerfaces 49 (2006) 71-78.

[31] E. H. Kim, X. D. Chen, D. Pearce, Colloids Surf. B: Biointerfaces, 26 (2002) 197-212.

[32] J. Fitzpatrick, K. Barry, P. Cerqueira, T. Iqbal, J. O'neill, Y. H. Roos, Int. Dairy J. 17 (2007) 383-392.

[33] J. Dupas, L. Forny, M. Ramaioli, J. Colloid Interface Sci. 448 (2015) 51-56.

[34] M. Hartmann, S. Palzer, Powder Technol. 206 (2011) 112-121.

[35] A. H. Nazemi, A. Majnooni-Heris, J. Colloid Interface Sci. 369 (2012) 402-410

[36] T. W. Y. Tham, X. Xu, A. T. H. Yeoh, W. Zhou, Food Chem. 218 (2017) 30-39.

[37] B.R. Nielsen, H. Stapclteldt, L. H. Skibsted, Int. Dairy J. 7 (1997) 589-599.

[38] F. Morales, M. A. J. S. van Boekel, Int. Dairy J. 8 (1999) 907-915.

[39] M. Rosenberg, S. L. Young, Food Struct. 12 (1993) 31-41.

[40] M. L. Vignolles, C. Lopez, M. N. Madec, J. J. Ehrhardt, S. Méjean, P. Schuck, R. Jeantet, J. Dairy Sci. 92 (2009) 58-70.

[41] J. M. Ames, Trends Food Sci. Tech. 1 (1990) 150-154.

[42] M. A. J. S. van Boekel, Mol. Nutr. Food Res. 45 (2001) 150-159.

[43] F. J. Morales, C. Romero, S. Jiménez-Pérez, J. Agric. Food Chem. 45 (1997) 1570-1573

[44] J. Gerrard, Aus. J. Chem. 55 (2002) 299-310.

[45] M. K. Haque, Y. H. Roos, J. Food Sci. 69 (2004) 23-29.

[46] E. Berlin, B. Anderson, M. Pallansch, J. Dairy Sci. 51 (1968) 1912-1915.

[47] H. S. Kim, A. J. Crosby, Adv. Mater. 23 (2011) 4188-4192.

[48] D. H. Chou, C. V. Morr, J. Am. Oil Chem. Soc. 56 (1979) 53-62.

[49] V. V. Mistry, H. N. Hassan, D. J. Robison, 11 (1992) 73-82.

[50] Y. Y. Xu, T. Howes, B. Adhikari, B. Bhandari, Dry. Technol. 31 (2013) 1939-1950.

[51] Y. Lei, Q. Zhou, Y. Zhang, J. Chen, S. Sun, I. Noda, J. Mol. Struct. 974 (2010) 88-93.

[52] A. B. McKenna, J. Dairy Res. 64 (1997) 423-432.

[53] N. Yazdanpanah, T. A. Langrish, Dry. Technol. 30 (2012) 1081-1087.

[54] A. Barth, Biochim. Biophys. Acta 1767 (2007) 1073-1101.

[55] D. M. Byler, H. Susi, Biopolymers 25 (1986) 469-487.

[56] K. Vinodhini, K. Srinivasan, Cryst. Eng. Comm. 17 (2015) 6376-6383.

Figures

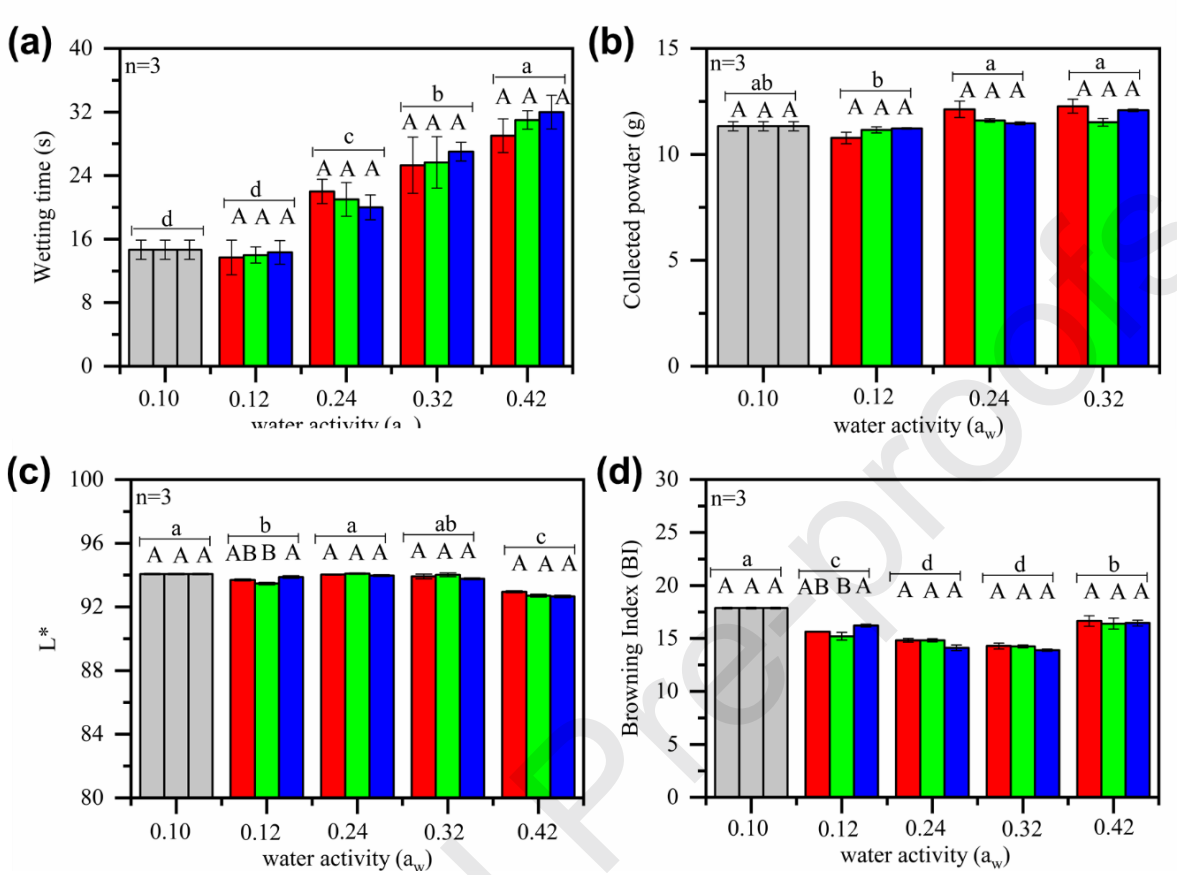

Figure 1. The profiles of (a) powder wettability, (b) collected powder mass (related to powder flowability), (c) lightness (L*), and (d) browning index (B1) of IF samples after storage under given water activity. Results on the effect of a_w are denoted with the given lowercase letter to indicate that they are not significantly different ($p>0.05$). Uppercase letters are used to indicate the effect of storage interval and results with the same letters are not significantly different. Error bars are standard errors (SE) of mean, while n represent the numbers of measurements. Gray refers to the reference powder (week 0). Red, green, and blue represent week 2, 4, and 6, respectively.

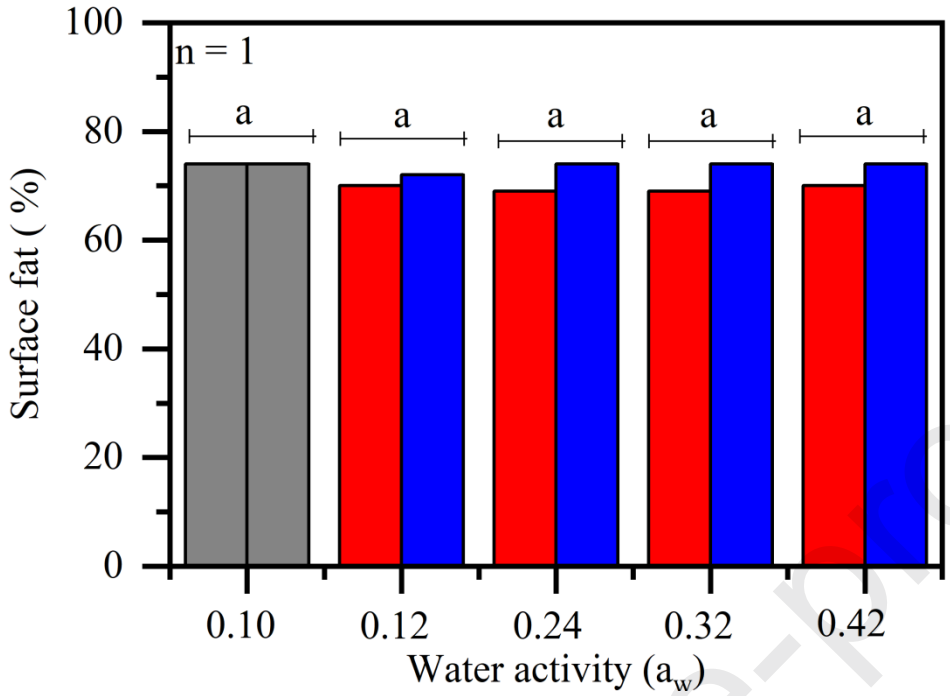

Figure 2. Surface fat of IF powders after storage at different values of water activity (a_w) after storage. The data with the same lowercase letters are not significantly different ($p>0.05$), while n represent the number of characterizations. Gray refers to the reference IF powder (week 0), while red and blue denote IF powder after week 2 and 6, respectively.

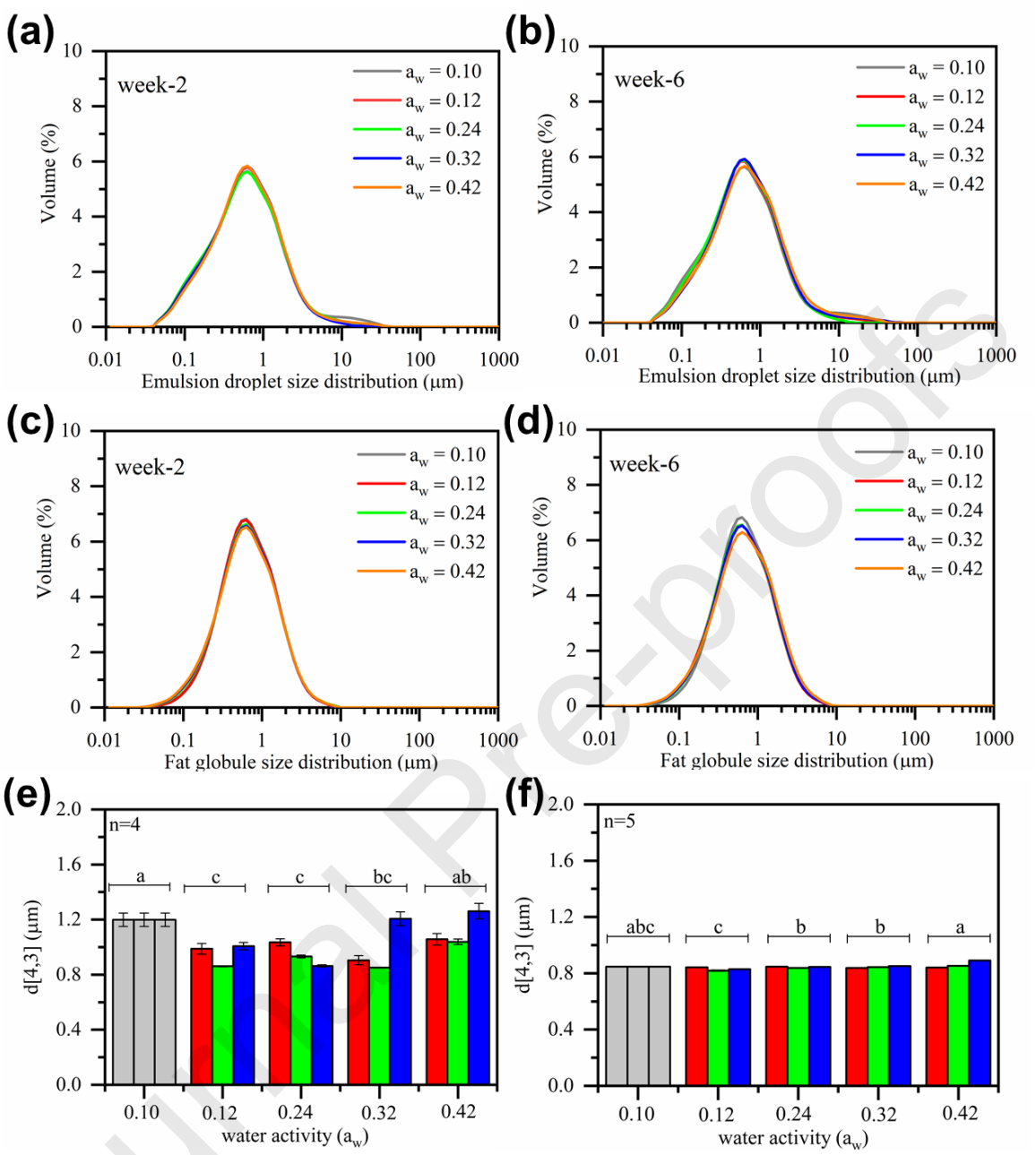

Figure 3. The particle size distribution and volume mean diameter (d[4,3]) of IF reconstituted samples (a, b, e) in the absence and (c, d, f) in the presence of 1 % EDTA + SDS after storage at given equilibrium water activity. Results on the effect of water activity are denoted with the given lowercase letter to indicate that they are not significantly different ($p>0.05$). Error bars are standard errors (SE) of mean, while n represent the numbers of measurements. Gray refers to the reference powder (week 0), while red, green, and blue represent the storage time of 2, 4, and 6 weeks, respectively.

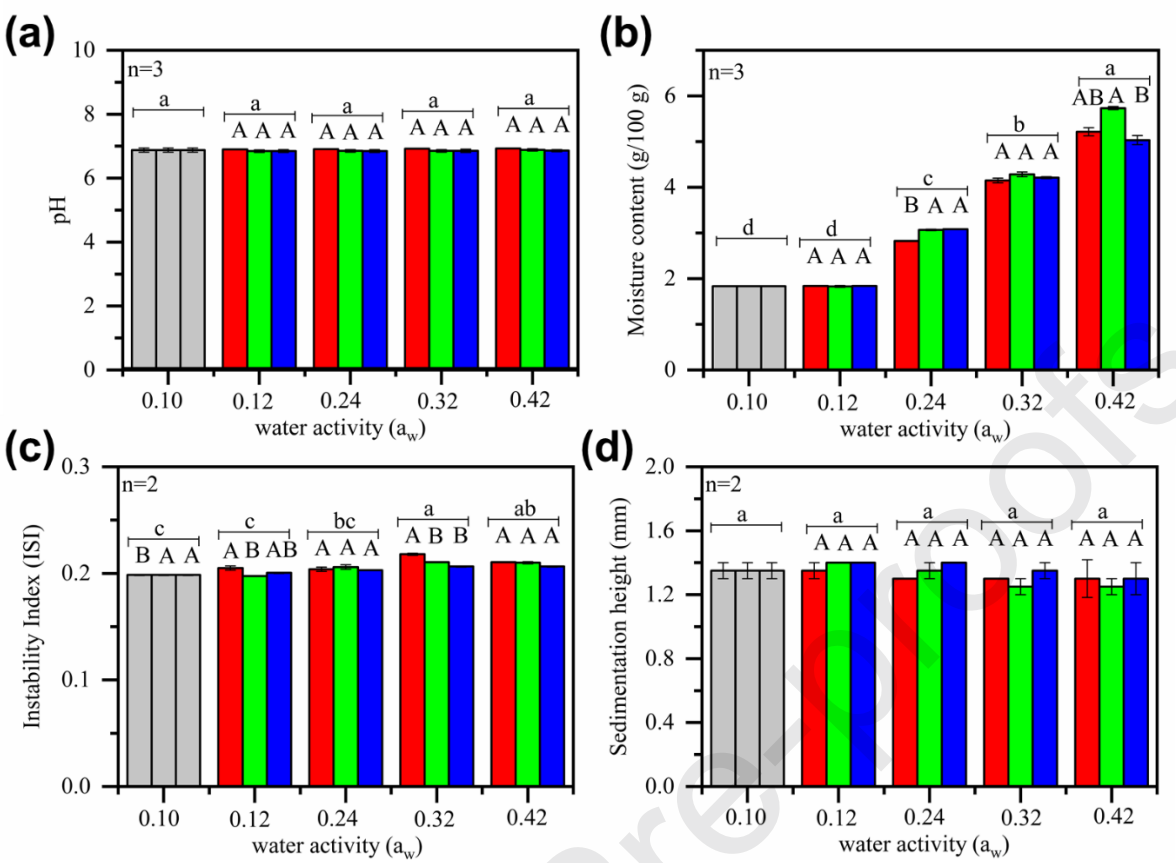

Figure 4. Bar plots for (a) pH, (b) moisture content, (c) instability index (ISI), and (d) sedimentation height of IF samples after storage under given water activity. Results on the effect of a_w are denoted with the given lowercase letter to indicate that they are not significantly different ($p>0.05$). Uppercase letters are used to indicate the effect of storage interval and results with the same letters are not significantly different. Error bars are standard errors (SE) of mean, while n represent the numbers of measurements. Gray refers to the reference powder (week 0). Red, green, and blue represent week 2, 4, and 6, respectively.

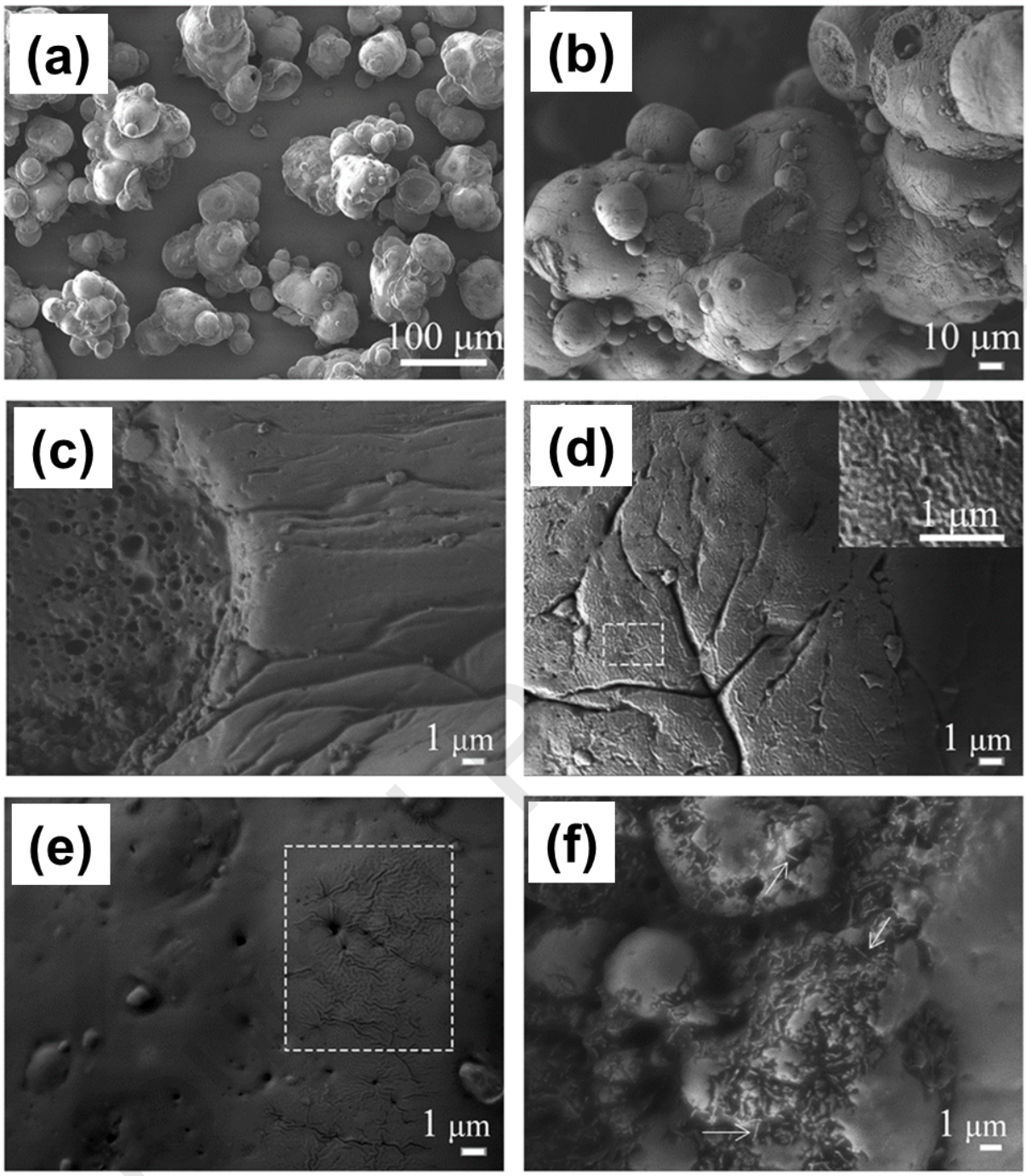

Figure 5. The morphology of IF powder at a_w = 0.12 corresponding to a magnification of (a) 150 x, (b) 500 x, and (c) 5000 x, also at (d) a_w = 0.24 and (e) a_w = 0.32, and the morphology of IF cake at (f) a_w = 0.42 after 6-week of storage. Inset figure: the magnification of wrinkled areas. White dotted square demonstrates wrinkles, while the white arrow shows the presence of needle-like lactose crystals on the particle surface.

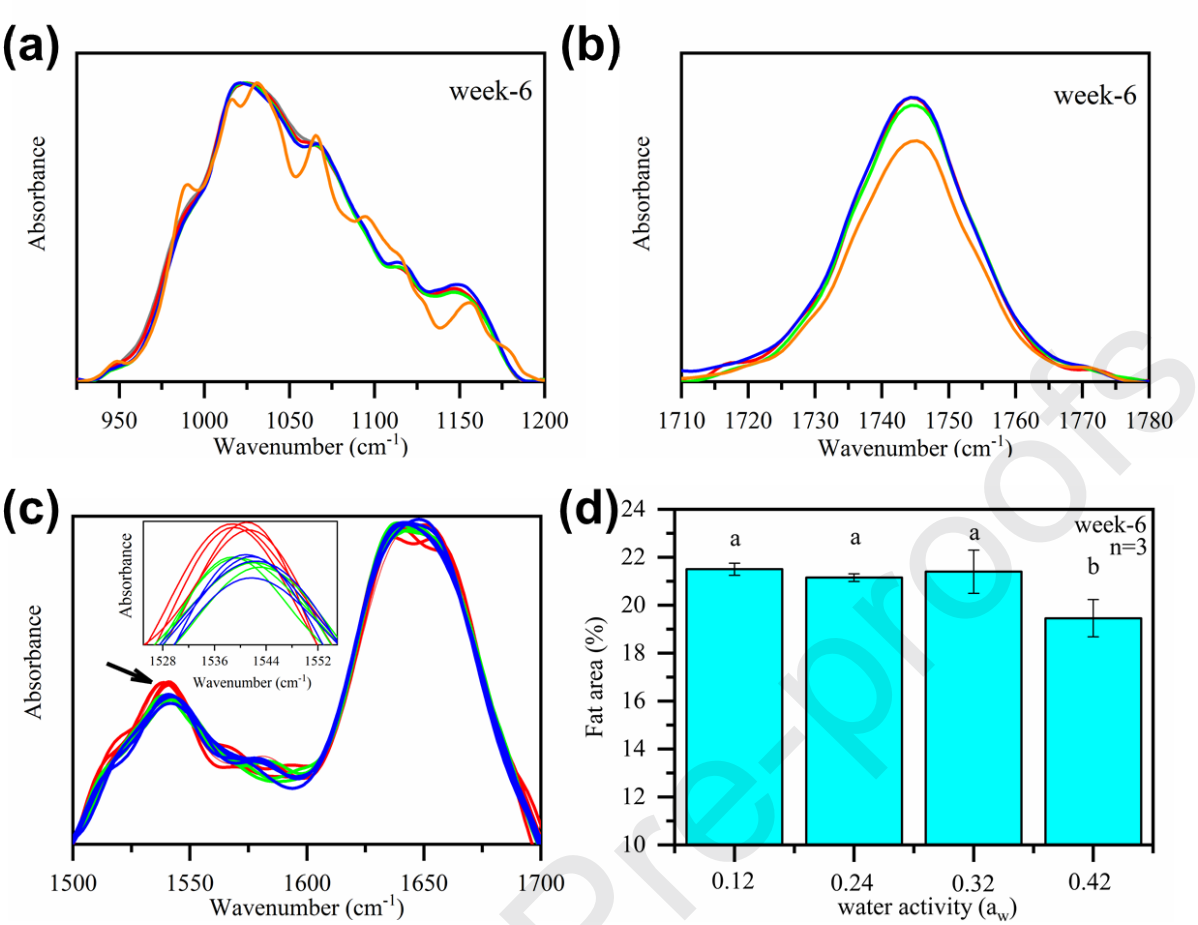

Figure 6. Representative IR absorption bands of (a) lactose and (b) fat), (c) Fourier self-deconvolution (FSD) of proteins, $n_{spectra}$ = 4, and (d) histogram analysis of fat migration of IF samples. When the effect of a_w is neglegible, a lower case letter is used ($p>0.05$). Error bars are standard errors (SE) of mean, while n represent the numbers of measurements. The black arrow denotes β-sheet. Inset: the magnification of β-sheet structure marked by arrow. Red, green, blue, and orange solid lines represent a_w = 0.12, 0.24, 0.32, and 0.42, respectively.

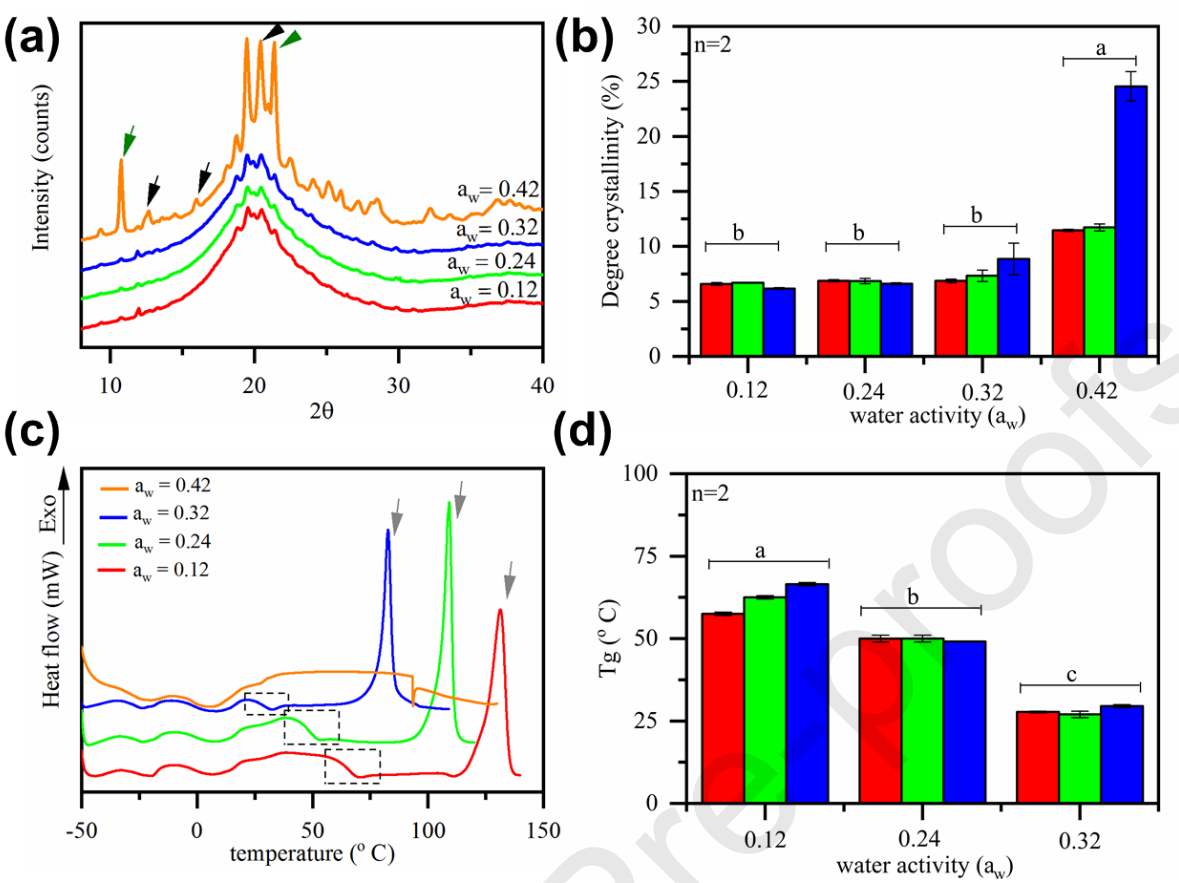

Figure 7. The profiles of (a) synchrotron X-ray diffraction (XRD), (b) degree of lactose crystallinity, effects of a_w are denoted with the given lowercase letter to indicate that they are not significantly different ($p>0.05$). Error bars are standard errors (SE) of mean, while n represent the numbers of measurements. The black and dark green arrows indicate the presence of α-lactose monohydrate and β-anhydrous lactose crystals, respectively. In addition, the black dotted square and gray arrow indicate the glass transition (Tg) and crystallization temperature (T_{cr}), respectively. Red, green, and blue represent week 2, 4, and 6, respectively.

Table 1. Measured water activity of IF samples during given storage periods

Targeted storage water activity (a_w)	Measured water activity (a_w)*		
	week 2	week 4	week 6
0.08	0.12±0.01	0.12±0.01	0.13±0.01
0.23	0.24±0.01	0.24±0.00	0.25±0.01
0.33	0.32±0.01	0.32±0.00	0.32±0.00
0.43	0.4±0.00	0.42±0.00	0.43±0.00

*number of measurements (n) = 3, mean ± standard error (SE)

Credit Author Statement

Robertus Wahyu N. Nugroho : Conceptualization, Formal analysis, Investigation, Writing – Original Draft

Marko Outinen : Conceptualization, Supervision, Resources, Writing – Review & Editing

Outi Toikkanen : Conceptualization, Supervision, Resources, Writing – Review & Editing

Antti Heino : Resources, Writing – Review & Editing

Daisuke Sawada : Formal analysis, Writing – Review & Editing

Orlando J. Rojas : Conceptualization, Supervision, Resources, Writing – Review & Editing, Funding acquisition

Graphical Abstract

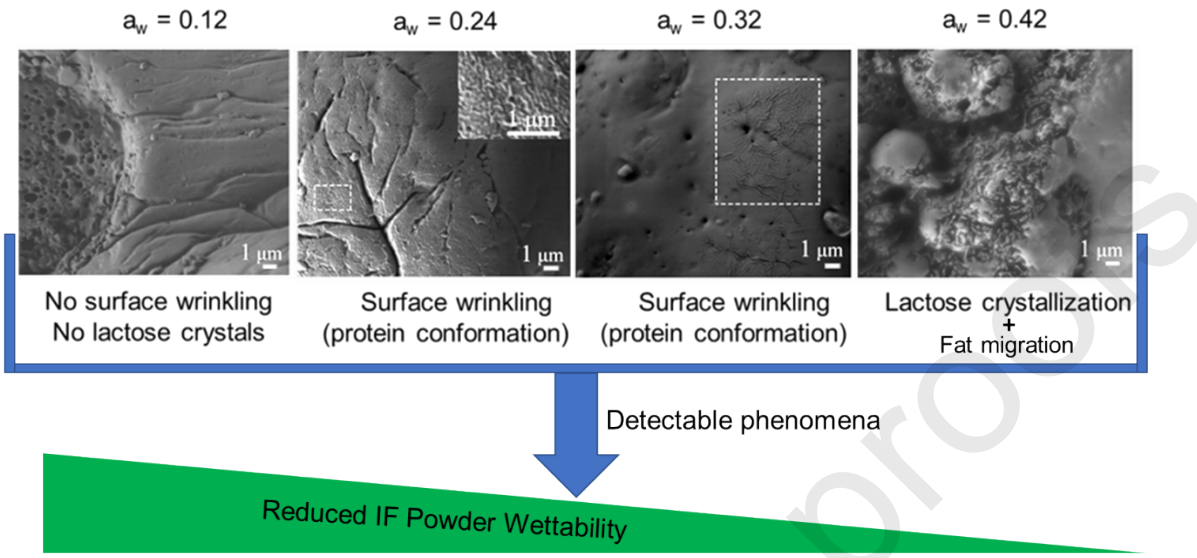

Highlights

- The wettability of infant formula (IF) powder deteriorates with increased water activity (a_w), even at $T_{storage} < T_g$.
- Lactose, fat, and protein are responsible for the changes in wettability at $a_w = 0.24 - 0.42$.
- Needle-like structures and changes in glass transition temperature (T_g), from amorphous to crystalline lactose, are significant at $a_w = 0.42$
- At low a_w, the morphology of powder and its surface, including wrinkling, tracked with changes in protein conformation.
- Except for wetting, no significant changes in the colloidal properties of IF powder ($a_w = 0.12 - 0.42$) are observed upon reconstitution.

Declaration of interests

☒ The authors declare that they have no known competing financial interests or personal relationships that could have appeared to influence the work reported in this paper.

☐The authors declare the following financial interests/personal relationships which may be considered as potential competing interests: